Analysis of Multi-Stage Joule-Thomson Microcoolers

H.S. Cao[1], P.P.P.M. Lerou[2], A.V. Mudaliar[1], H.J. Holland[1], J.H. Derking[1], D.R. Zalewski[1], H.J.M. ter Brake[1]

[1]University of Twente, 7500 AE Enschede, The Netherlands
[2]Kryoz Technologies,7521 PV Enschede, The Netherlands

ABSTRACT

Microcoolers machined from glass wafers based on Joule-Thomson (J-T) expansion have been investigated for many years at the University of Twente. After successful development of single-stage J-T microcoolers with a cooling capacity of around 10 mW at 100 K, research is being carried out to attain lower temperatures to 30 K using multiple stages. As an initiative in this research effort, a simplified dynamic model of a two-stage microcooler has been developed using Matlab® to analyze the cooler performance. The first stage operates with nitrogen as the working fluid from 80 bar high pressure to 6 bar low pressure and is used to precool the second stage. The second stage operates with neon from a high pressure of 40 bar to a low pressure of 1 bar. The model is composed of single lumped heat capacities at both the evaporators and the precooler. These capacities are linked via thermal resistances and are cooled by the evaporating fluids. The effect of the counter-flow heat exchanger (CFHX) length on the performance of the two-stage microcooler is discussed. The length of the CFHX in the second stage between precooler and evaporator is very critical regarding the cool-down time. Based on the model, a preliminary design is made with the envelope dimensions of 8.30 x 37.00 x 0.72 mm that has a cooling power of 5 mW at 27 K. It cools down in less than 3 hours with a corresponding mass flow rate of 2.6 mg/s of nitrogen and 1.5 of mg/s neon.

INTRODUCTION

Devices such as infrared detectors, low-noise amplifiers and superconducting devices require a low temperature and little cooling power with a range of a few milliwatts.[1,2] Most of these devices need temperatures lower than 100 K. The temperature range (from room temperature to the operating temperature) is too large for a single-stage cooler. A large temperature range results in a large pressure range in the cycle which puts forward higher requirements for the compressor. One way of dealing with this situation is to implement a multi-stage cooling process. In addition, the efficiency can be increased via multi-staging.

Since the 1980s, several attempts have been made to build a micro refrigerator to cool the above-mentioned devices.[3,4] At the University of Twente, research on microcoolers has been investigated for many years. Burger et al.[5] investigated how to build a small cryocooler via micromechanical techniques. Lerou et al.[6-8] designed and produced microcoolers with cooling powers of about 10-20 mW at 100 K. Currently, our research is focused on developing single-stage coolers with higher cooling powers and incorporating sorption compressors.[9] Also, the development of multistage microcoolers

Cryocoolers 16, edited by S.D. Miller and R.G. Ross, Jr.

is investigated. This paper presents the analysis of a two-stage microcooler for cooling power of 5 mW at around 30 K.

TWO-STAGE MICROCOOLER MODEL

A simplified model of a two-stage microcooler based on the Linde-Hampson cooling cycle has been developed and is shown Figure 1. In the first stage, nitrogen is used as the working fluid with a high pressure of 80 bar and a low pressure of 6 bar. The first stage is used to precool the second stage that operates with neon at a high pressure of 40 bar and a low pressure of 1 bar. The model is composed of single lumped heat capacities at the evaporators and at the precooler. Each evaporator is assumed to have a heat capacity equal to that of the evaporator material plus half of the counter-flow heat exchanger (CFHX) adjacent to it. The lumped element heat capacity of the precooler is the sum of the heat capacity of the precooler itself and half of each of the adjacent CFHXs. The CFHXs are assumed to have no heat capacity other than the above-mentioned lumped capacity elements. These capacities are linked via thermal resistances and are cooled by the evaporating fluids.

The two-stage microcooler lumped model is expressed by the following energy balances:

$$\dot{m}_l h_l^{pH,in} + \dot{Q}_{loadI} + \dot{Q}_{pre} - \dot{m}_l h_l^{pL,\,out} = C_l \frac{dT_{evapl}}{dt} \tag{1}$$

$$\dot{m}_H h_2^{pH,in} + \dot{m}_H h_3^{pL,out} + \dot{Q}_{load3} - \dot{m}_H h_2^{pL,out} - \dot{m}_H h_3^{pH,in} - \dot{Q}_{pre} = C_3 \frac{dT_{pre}}{dt} \tag{2}$$

$$\dot{m}_{ll} h_3^{pH,in} + \dot{Q}_{load2} - \dot{m}_{ll} h_3^{pL,out} = C_2 \frac{dT_{evapll}}{dt} \tag{3}$$

where $\dot{m}_l$ and $\dot{m}_{ll}$ are mass flow rates of the first and the second stage. $\dot{Q}_{load1}$, $\dot{Q}_{load2}$ and $\dot{Q}_{load3}$ are thermal loads from the microcooler environment, and $\dot{Q}_{pre}$ is the conductive heat flow from the

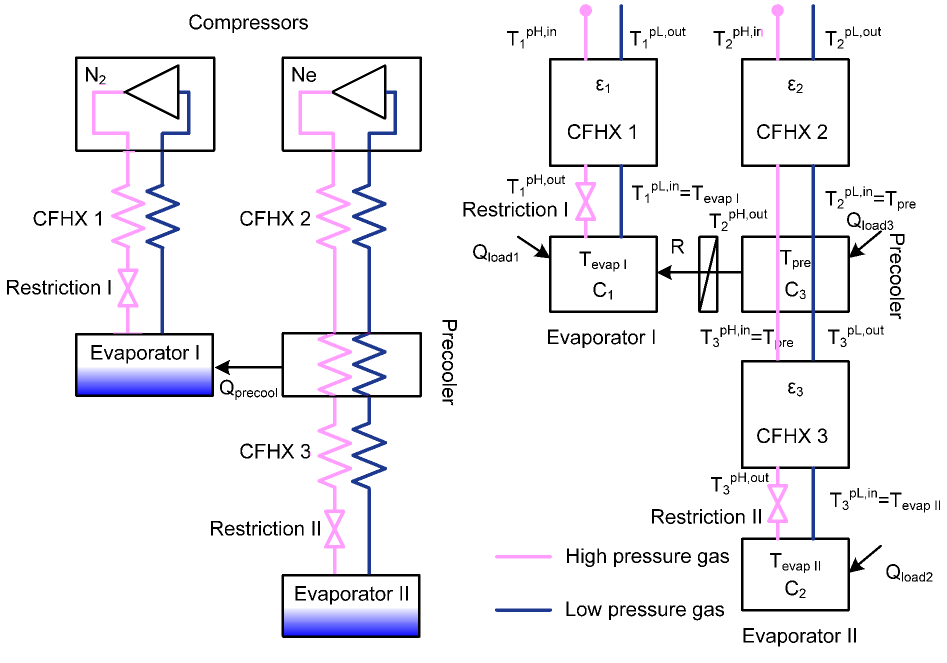

Figure 1. Schematic diagram of the two-stage microcooler (left) and lumped-element model (right). ε_1, ε_2, ε_3 - heat exchanger efficiencies of CFHX 1, CFHX 2, CFHX 3; R - thermal resistance between precooling stage and evaporator *l*; C_1 - heat capacities of evaporator *I* and half of CFHX 1; C_2 - heat capacities of evaporator II and half of CFHX 3; C_3 - heat capacities of precooler, half of CFHX 2 and half of CFHX 3.

precooler to evaporator l. Because the emissivity of glass is relatively large, the cooler's surface is covered with a thin gold layer to decrease radiation losses. Emissivity of a smooth gold layer is in the order of 0.02.[10] T_{pre}, T_{evapI} and T_{evapII} are the temperatures of precooler and the evaporators, respectively. *h* refers to enthalpy, and *in*, *out*, *pH* and *pL* refer to inlet, outlet, high pressure line and low pressure line, respectively. C_1, C_2 and C_3 are the heat capacities of the three lumped elements. As mentioned above, the CFHXs have no heat capacity other than their contribution to the lumped elements at the evaporators and the precooler. In the model, each CFHX is fully characterized by its efficiency as follows:

$$\varepsilon_{\mathrm{i}} = \frac{T_{\mathrm{i}}^{\mathrm{pL,out}} - T_{\mathrm{i}}^{\mathrm{pL,in}}}{T_{\mathrm{i}}^{\mathrm{pH,in}} - T_{\mathrm{i}}^{\mathrm{pL,in}}} \tag{4}$$

where *i* refers to the number the CFHX shown in Fig. 1.

This CFHX efficiency, however, is flow dependent. Since the mass flow rate varies during cool down, the efficiency has to be expressed in terms of the mass flow rate. The efficiency estimated from steady-state is used as a reference. Given certain geometry, the CFHX performance in steady-state was evaluated via the static model introduced by Lerou at al.[10]. Equation (4) yields the steady-state efficiency ε_∞ with steady-state mass flow rate $\dot{m}_\infty$. The efficiency during cool-down as a function of mass flow rate $\dot{m}$ appears to be approximated by

$$\varepsilon = 1 - \left(1 - \varepsilon_\infty\right)^{\beta} ; \beta = \left(\dot{m}_\infty / \dot{m}\right)^{0.54} \tag{5}$$

The temperature boundary conditions for the CFHXs are:

$$\begin{aligned} T_1^{\mathrm{pH,in}} &= T_2^{\mathrm{pH,in}} = 300\,\mathrm{K} \\ T_1^{\mathrm{pL,in}} &= T_{\mathrm{evapI}} \\ T_2^{\mathrm{pL,in}} &= T_3^{\mathrm{pH,in}} = T_{\mathrm{pre}} \\ T_3^{\mathrm{pL,in}} &= T_{\mathrm{evap\,II}} \end{aligned} \tag{6}$$

Because of the small dimensions of the restriction and a low mass flow rate, the flow through the restriction is laminar. Furthermore, we assume the evaporator to be isothermal at a temperature equal to that of the evaporator, because the evaporator is in direct thermal contact with the restriction.[6, 7] In that case, the mass flow rate is given by the following equation[10, 11],

$$\dot{m}\left(T_{\mathrm{evap}}\right) = \frac{1}{12}\frac{wh^3}{l}\int_{pL}^{pH}\frac{\rho\left(p, T_{\mathrm{evap}}\right)}{\mu\left(p, T_{\mathrm{evap}}\right)}dp \tag{7}$$

where *w*, *h* and *l* are width, height and length of the restriction, *pH* and *pL* are the high and low pressure respectively, $\rho\,(p,T_{\mathrm{evap}})$ and $\mu\,(p,T_{\mathrm{evap}})$ are density and viscosity as a function of pressure and temperature, respectively.

TWO-STAGE MICROCOOLER GEOMETRY

The geometry of the two-stage microcooler is based on a design that was realized by Lerou et al.[8] These coolers consist of a stack of three glass wafers. The high and low pressure lines are etched as rectangular channels in the top and bottom wafers. The high pressure line ends in a flow restriction, which is connected to the low pressure line by an evaporator volume . Thus, a CFHX is formed by the high and low pressure channels and the thin intermediate glass wafer. The two stages are assumed to be placed side-by-side as schematically shown in Fig. 1 as described by Lerou et al.[8] CFHX 1 is assumed to be thermally isolated from CFHX 2, whereas the precooler in between CFHX 2 and CFHX 3 is assumed to be in direct thermal contact with evaporator. The thermal resistance between these two components is fully determined by the glass of the separating walls. In the geometry that we consider, the height of the three-wafer stack is 0.72 mm and the channels are 50 ìm high. The intermediate glass wafer in the CFHXs has a thickness of 0.10 mm. Further parameters are given in Table. 1. In the present study, the length of the CFHXs varies.

Table 1. Two-stage microcooler geometry (dimensions in mm except for restriction height).

	CFHX Length	CFHX width	Channel width
CFHX 1	20.00~35.00	5.00	4.00
CFHX 2	10.00~25.00	3.33	2.67
CFHX 3	5.00~20.00	3.33	2.67
	Length	Outside width	Inside width
Evaporator I	3.50	5.00	4.00
Evaporator II and precooler	3.50	3.33	2.67
	Length	Width	Height (μm)
Restriction I	1.00	0.40	1.10
Restriction II	2.00	0.70	1.10

RESULTS AND DISCUSSION

Effect of CFHX Length

The most important optimization parameters of a microcooler CFHX are its length and the thickness of the intermediate glass wafer. The latter should be as small as possible but is limited to 0.10 mm due to manufacturing limitations. Therefore, we specifically investigated the effect of the length of the CFHXs. Based on the relation between efficiency and mass flow rate, the effect of CFHX length on the cooler performance was analyzed. Two of the three CFHX lengths are fixed whereas the target one is varied.

The change in length of CFHX 1 from 20 to 35 mm increases the gross cooling power of the first stage from 36.1 mW to 38.4 mW due to an increase in the efficiency. Subtracting the precooling power and the parasitic heat loads, a net cooling power remains available at the first-stage evaporator as depicted in Figure 2. The net cooling power reaches its maximum at a length of 25 mm as shown in Figure 2. There is no gain in net cooling power with increase in the length of CFHX 1 from 25 to 35 mm due to an increase in radiation losses and precooling power. Fig. 2 also shows the net cooling power at the second stage, which is almost constant. The CFHX length affects the cool-down time because of increased heat capacity from 5.2 hours to 5.5 hours, although not substantially.

When the length of CFHX 2 is changed from 10 to 25 mm with CFHX 1 and CFHX 3 fixed at 25 mm and 15 mm, respectively, the gross cooling power at the first stage is constant (37.5 mW) but the net power appears to increase as shown in Figure 2. The reason is that the outlet temperature of the high-pressure flow of CFHX 2 decreases with increasing length (higher efficiency). Therefore, less power is needed for precooling.

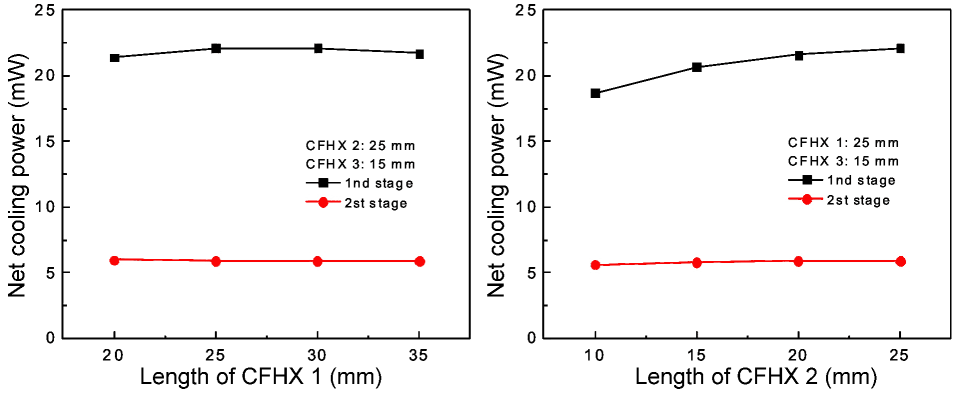

Figure 2. Effect of the CFHX length on the net cooling (left: CFHX 1, right: CFHX 2).

Varying the length from 5 to 20 mm with CFHX 1 and CFHX 2 both fixed at 25 mm slightly affects the net cooling power of the first stage as shown in Figure 3. However, the net cooling power of the second stage is significantly affected because of the changing CFHX efficiency and parasitic heat load. At a length of 5 mm, the cooler does not reach a stable low temperature at all. The length of CFHX 3 also markedly influences the cool-down time as shown in Figure 3 which is due to the changing heat capacity.

Cooler Performance with Fixed CFHX Length

Based on the study of CFHX length, a length of 20 mm for CFHX 1 and 2 was chosen when CFHX 3 is 10 mm long. The dynamic behavior of this preliminary design is studied in detail. The temperatures of both evaporators and precooler versus time are shown in Figure 4 where the cool-down times of the first stage and the second stage are 0.34 hr and 2.83 hr, respectively. The rapid increase of precooler temperature at 2.83 hr is induced by the significant rise of mass flow rate of the second stage as shown in Figure 5. The mass flow rate depends on fluid viscosity and density according to Eq. 7. Thus, the mass flow rate rise can be explained by a change in fluid property with evaporator temperature. After the evaporator temperature has reached the boiling temperature, the mass flow rate of the first stage stabilizes at around 2.6 mg/s while the second stage remains steady at about 1.5 mg/s. The cooling powers (gross and net) at both stages are shown in Figure 6. The net cooling power of the second stage stabilizes at 5.0 mW meeting the design requirements. The peaks in the gross cooling power of the first stage and the second stage are induced by the peaks in mass

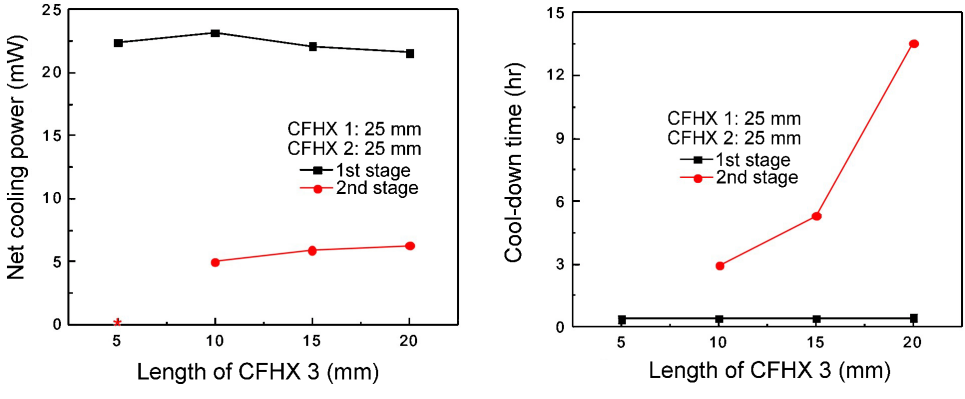

Figure 3. Effect of CFHX 3 length on the net cooling power (left) and cool-down time (right).

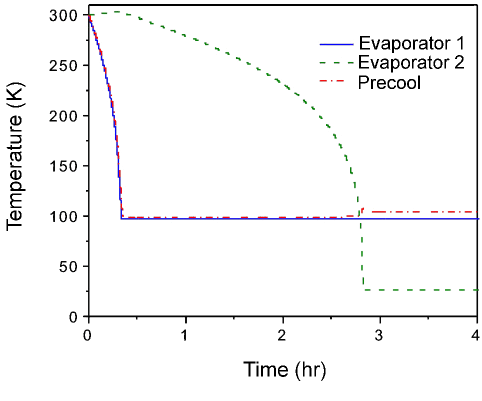

Figure 4. Temperature versus time of both evaporators and precooling stage.

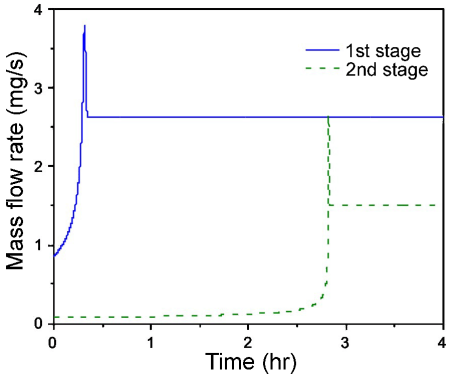

Figure 5. Mass flow rate versus time for both cooler stages.

flow rates of both stages. As a further effect of the peaking mass flow rate, the first-stage evaporator cools down relatively quickly and the temperature difference between evaporator *1* and the precooler increases. As a result, the conductive heat flow from precooler to evaporator *1* increases, thereby decreasing the net cooling power of the first stage. This explains the first dip in the net cooling power coinciding with the peak in the gross cooling power at the first stage. The drop of the net cooling power of the first stage at 2.83 hr is induced by the increasing precooling power because of the rise of mass flow rate of the second stage.

CONCLUSIONS

A simple lumped-element model was developed for a two-stage microcooler. The first stage operates with nitrogen as the working fluid from 80 bar high pressure to 6 bar low pressure. The first stage cooler is used to precool the second stage which operates with neon, from a high pressure of 40 bar to a low pressure of 1 bar. The effect of the CFHX length on the cooler performance is specifically investigated. The CFHX adjacent to the evaporator of the second stage is critical in determining the cool-down time and net cooling power. With an increase in length, the cool-down time increases, and with the decrease in length, the net cooling power decreases. A preliminary design was made with overall dimensions of 8.30 x 37.00 x 0.72 mm that has a cooling power of 5 mW at 27 K. It cools down less than 3 hours with corresponding mass flow rate of 2.6 mg/s of nitrogen and 1.5 mg/s of neon. Future research will be focused on more detailed modeling of this preliminary design by integrating with full CFHX model.

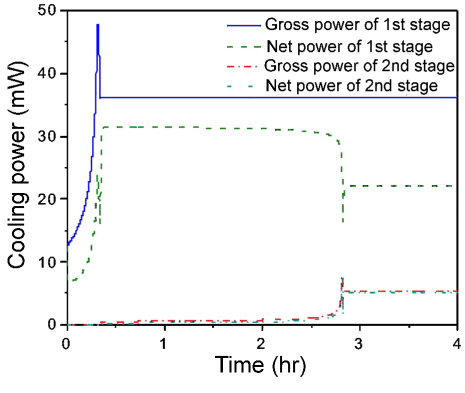

Figure 6. Gross and net cooling powers versus time for both cooler stages.

ACKNOWLEDGMENT

This work is supported by the Dutch Technology Foundation (STW), the European Space Agency and the UT research institute IMPACT.

REFERENCES

1. Little, W.A., “Microminiature Refrigeration - Small is Better,” *Physica*, vols 109-110B (1982), pp. 2001-2009.
2. Fung, C.W., Kwok, W.Y., “Structural Analysis of High-Tc Cuprate Superconductors,” *J. Supercond.*, vol. 4 (1991), pp. 415-422.
3. Little, W.A., “Microminiature refrigeration,” *Rev. Sci. Instrum.*, vol 55 (1984), pp. 661–680.
4. Chorowski, M., Bodio, E., Wilczek, M., “Development and testing of a miniature Joule-Thomson refrigerator with sintered powder heat exchanger,” *Adv. in Cryogenic Engineering,* Vol. 39B, Plenum Publishing Corp., New York (1994), pp. 1475-1481.
5. Burger, J.F., "Cryogenic microcooling, A micromachined cold stage operating with a sorption compressor in a vapor compression cycle," PhD dissertation, University of Twente, Enschede, 2001.
6. Lerou, P.P.P.M., Venhorst, G.C.F., Berends, C.F., Veenstra, T.T., Blom, M., Burger, J.F., ter Brake, H.J.M., and Rogalla, H., “Fabrication of a micro cryogenic cold stage using MEMS-technology,” *J. Micromech. Microeng*., vol. 16 (2006), pp. 1919–1925.
7. Lerou, P.P.P.M., ter Brake, H.J.M., Burger, J.F., Holland, H.J. and Rogalla, H., “Characterization of micromachined cryogenic coolers,” *J. Micromech. Microeng*., vol. 17 (2007), pp. 1956-1960.
8. Lerou, P.P.P.M., ter Brake, H.J.M., Jansen, H.V., Burger, J.F., Holland, H.J., Rogalla, H., “Micromachined Joule-Thomson coolers,” *Adv. in Cryogenic Engineering*, Vol. 53, Amer. Institute of Physics, Melville, NY (2008), pp. 614-621.
9. Derking, J. H., Zalewski, D. W., Garcia, M., Holland, H.J., Mudaliar, A. V., Cao, H. S., Lerou, P.P.P.M., ter Brake, H.J.M., “Progress in Joule-Thomson microcooling at the University of Twente,” *Cryocoolers 16*, ICC Press, Boulder, CO (2011), (this proceedings).
10. Bejan, A., *Heat Transfer*, John Wiley & Sons New York, 1993. ISBN 0-471-50290-1.
11. Lerou, P.P.P.M., Veenstra, T.T., Burger, J.F., ter Brake, H.J.M., Rogalla, H., “Optimization of counterflow heat exchanger geometry through minimization of entropy generation,” *Cryogenics*, Vol. 45, Issues: 10-11, October-November 2005, pp. 659-669.